IMA Journal of Mathematics Applied in Medicine & Biology (1986) **3**, 191–210

Hopf Bifurcation in Host–Parasitoid Models

H. A. LAUWERIER

Centre for Mathematics and Computer Science, P.O. Box 4079, 1009 AB Amsterdam, The Netherlands

AND

J. A. J. METZ

Institute of Theoretical Biology, Groenhovenstraat 5, 2311 BT Leiden, The Netherlands

[Received 2 January 1986 and in revised form 25 June 1986]

For a wide class of host–parasitoid models, a reduction to Arnold's normal form can be carried out in an explicit way. In the case of Hopf bifurcation, the shape and size of the elliptic limit curve can be derived in terms of the parameters of the model. Some models have a rich bifurcation behaviour with both supercritical and subcritical Hopf bifurcation, and with a transition zone in the parameter plane for which there exists a pair of limit curves, one stable and one unstable. The theory is confirmed and illustrated by numerical experiments.

1. Introduction

OVER the past years, the second author did a number of intriguing computer experiments in connection with host–parasitoid models of the kind

$$x_{n+1} = x_n \phi(y_n), \qquad y_{n+1} = a x_n - x_{n+1}, \quad a > 1, \tag{1.1}$$

where x_n and y_n are the numbers of hosts and parasitoids of generation n. The function $\phi(y)$ is assumed to be differentiable with $\phi'(y) < 0$, $\phi(0) = a$, and $\phi(\infty) < 1$. The function $\phi(y)$ contains a second parameter $b > 0$, which enables us to study bifurcation phenomena with respect to the non-trivial equilibrium for various combinations of a and b in the parameter plane. It is perhaps of interest to note that the iterative process (1.1) is invertible with

$$x_n = (x_{n+1} + y_{n+1})/a, \qquad y_n = \phi^{-1}\big(a x_{n+1}/(x_{n+1} + y_{n+1})\big).$$

We considered in particular the so-called Hassell–Varley (HV) model and a new model in which interaction between parasitoids was taken into account, the so-called parasitoid–parasitoid interaction (PP) model (Vaz Nunez, 1977; Lubberhuizen, 1983). The HV-model showed the usual characteristics of Hopf bifurcation in the unstable part of the parameter plane. However, the bifurcation behaviour of the PP model appeared to be much more complicated. Instead of a single invariant curve—the Hopf circle—two such curves could be present, one attracting and the other repelling. For some parameter values there was no such curve. The second author succeeded in giving a qualitative explanation of his

findings, based upon the theory of normal forms. In this paper, these ideas are worked out in a quantitative way. Our results can also be applied to a recent model proposed by Hassell (1984). This model appears to have the same complicated bifurcation behaviour as the PP model.

Leaving aside the trivial equilibrium $x = y = 0$, there exists a single non-trivial equilibrium

$$x = \frac{c}{a-1}, \qquad y = c,$$

with c as the unique root of $\phi(c) = 1$. For a certain line in the parameter plane, the eigenvalues λ and $\bar{\lambda}$ are complex and of modulus one. Across this line, the so-called Hopf line, we may expect Hopf bifurcation. Close to the Hopf line we may write

$$\lambda = (1+\mu)e^{i\alpha}, \qquad 0 < \alpha < \pi,$$

where μ is a small quantity, the bifurcation parameter. In the special cases considered in this paper, the parameters μ and α are in a 1–1 correspondence with the model parameters a and b. Thus the Hopf line corresponds to a part of the unit circle in the complex λ plane. The eigenvalue equation of the non-trivial equilibrium is of the form

$$\lambda^2 - \lambda(1 + L/a) + L = 0, \tag{1.2}$$

where $L = -ac\phi'(c)/(a-1)$. At the line we have $L = 1$ so that $\lambda + \bar{\lambda} = 1 + 1/a$. This gives $\cos\alpha = \frac{1}{2}(1 + 1/a)$. Since $1 < a < \infty$, the value of α is restricted to the interval $(0, \frac{1}{3}\pi)$. Thus a periodic solution of (1.1) would imply a period larger than 6. We state this as a theorem.

THEOREM *For any periodic solution of a model of the class* (1.1), *the period is larger than six.*

Of course this theorem only applies at the Hopf line. Numerically it turns out that, further away from the Hopf line, the period only increases. The reason is that when the Hopf circle enlarges it comes nearer to the saddle point at the origin, and in this region the system takes only small steps. Also, the theorem holds more generally for models handling time effects, characterized by

$$x_{n+1} = x_n \psi(x_n, y_n), \qquad y_{n+1} = ax_n - \psi(x_n, y_n),$$

with $\dfrac{\partial\psi}{\partial x} \geqslant 0$ and $\dfrac{\partial\psi}{\partial y} < 0$.

According to the theory of normal forms, the two-dimensional map (1.1) can be written in the form

$$z_{n+1} = \lambda z_n + A_{21} z_n^2 \bar{z}_n + \hbar_n, \tag{1.3}$$

where z and $\bar{z}$ are local complex coordinates at the equilibrium and where $\hbar_n$ denotes terms of higher order. The constant A_{21}, taken at $\mu = 0$, is an essential parameter of the model. In the plane determined by the conjugate complex

variables z and $\bar{z}$, we have an invariant circle, the Hopf circle, with its radius R given by

$$\mu/R^2 = \mathrm{Re}\,(-\mathrm{e}^{-\mathrm{i}\alpha}A_{21}).$$

For the original variables (x, y), this corresponds to an invariant curve of elliptical shape surrounding the equilibrium point. If $\mu/R^2 > 0$ we have supercritical Hopf bifurcation, with an attracting invariant curve around an unstable equilibrium ($\mu > 0$). If $\mu/R^2 < 0$ we have subcritical Hopf bifurcation, with a repelling invariant curve around a stable equilibrium ($\mu < 0$). In some models there exists a critical value α_0 for which $\mathrm{Re}\,(\mathrm{e}^{-\mathrm{i}\alpha_0}A_{21}) = 0$. Close to this critical value there is a bifurcation of a more complicated kind, which we called 'crater bifurcation'. It is characterized by the simultaneous occurrence of a stable and of an unstable invariant curve. A sketch of the mathematical theory will be given in the Appendix.

In this paper, the reduction of (1.1) to its normal form (1.3) is carried out in an explicit way. If $\phi(y)$ has, at the equilibrium value, the Taylor expansion

$$\phi\big(c(1+t)\big) = 1 - At + ABt^2 - ACt^3 + \ldots, \tag{1.4}$$

with (at the Hopf line) $A = 1 - 1/a$, then the following results have been obtained. The radius R of the Hopf circle in the $(z, \bar{z})$ plane is given by

$$\frac{2\mu}{R^2} = A - (A+1)B + 4B^2 - 3C. \tag{1.5}$$

The corresponding ellipse in the original (x, y) plane is given by

$$a(a-1)\,\mathrm{d}x^2 - (a-1)\,\mathrm{d}x\,\mathrm{d}y + \mathrm{d}y^2 = (3a+1)c^2R^2/a,$$

where $(\mathrm{d}x, \mathrm{d}y)$ are local coordinates at the equilibrium $x = c/(a-1)$, $y = c$. This theory will be applied to the following few special cases.

S: $\phi(y) = \dfrac{a}{1+y^b}$,

HV: $\phi(y) = a\exp(-y^b)$ (Hassell & Varley, 1969),

PP: $\phi(y) = a\exp\left(-\dfrac{(1+y)^{\frac{1}{2}} - 1}{b}\right)$ (Metz, Vaz Nunez, 1977),

H: $\phi(y) = a[\theta\mathrm{e}^{-y} + (1-\theta)\mathrm{e}^{-by}]$ (Hassell, 1984).

The main results are as follows.

S-model: Unstable for $b > 1$; Hamiltonian for $b = 1$ on a logarithmic scale; no Hopf bifurcation; formally, $R = \infty$ for all values of a.

HV model: Supercritical Hopf bifurcation for all a.

PP model: Supercritical Hopf bifurcation for $a > 3{\cdot}85$ and subcritical Hopf bifurcation for $a < 3{\cdot}85$.

H model: As in the previous model; if $\theta = \frac{1}{2}$ there is supercritical Hopf bifurcation for $a > 2{\cdot}29$ and subcritical Hopf bifurcation for $a < 2{\cdot}29$.

2. Reduction to the normal form

In this section, the reduction of (1.1) to the normal form (1.3) will be carried out explicitly. The first step is the use of a new variable

$$w = x\phi(y). \tag{2.1}$$

Then (1.1) can be replaced by

$$x_{n+1} = w_n, \qquad w_{n+1} = w_n\phi(ax_n - w_n). \tag{2.2}$$

Let λ and $\bar{\lambda}$ be the eigenvalues of the equilibrium as determined by (1.2). Then, by a linear transformation, (x, w) can be replaced by complex coordinates $(z, \bar{z})$, where z is an eigenvector associated to λ. Explicitly,

$$cz = a\sigma(\bar{\lambda}x - w) - c_0, \qquad c\bar{z} = a\bar{\sigma}(\lambda x - w) - \bar{c}_0, \tag{2.3}$$

where σ is a scaling factor and where c_0 is determined by the condition

$$z = 0 \quad \text{for } x = w = c/(a-1).$$

The factor σ is chosen in such a way that

$$ax - w = c(1 + z + \bar{z}). \tag{2.4}$$

In the eigenvector coordinates $(z, \bar{z})$, the map (2.2) takes the form

$$z_{n+1} = \lambda z_n + a_{20}z_n^2 + a_{11}z_n\bar{z}_n + a_{02}\bar{z}_n^2 + \text{h}_n, \tag{2.5}$$

and a similar relation with conjugate complex quantities. From (2.3) we obtain

$$cz_{n+1} = a\sigma(\bar{\lambda}x_{n+1} - w_{n+1}) - c_0 = a\sigma w_n[\bar{\lambda} - \phi(ax_n - w_n)] - c_0,$$

so that, in view of (2.4),

$$cz_{n+1} = a\sigma w_n[\bar{\lambda} - \phi(c(1 + z_n + \bar{z}_n))] - c_0.$$

From (2.3) we obtain by inversion a relation of the kind

$$w = \frac{c}{a-1}(1 + c_1z + c_2\bar{z}).$$

Using also the expansion (1.4), we obtain

$$z_{n+1} = \frac{a\sigma}{a-1}\{(1 + c_1z_n + c_2\bar{z}_n)[\bar{\lambda} - 1 + A(z_n + \bar{z}_n) - AB(z_n + \bar{z}_n)^2 + AC(z_n + \bar{z}_n)^3 + \cdots] - (\bar{\lambda} - 1)\},$$

which is identical with (2.5). Although $\lambda = (1 + \mu)e^{i\alpha}$ we need the coefficients a_{20}, a_{11}, a_{02}, etc. only at the Hopf line where $\mu = 0$. Then the calculation may be simplified somewhat. We have

$$A = 1 - 1/a = 2(1 - \cos\alpha), \qquad c_1 = 1 - \bar{\lambda}, \quad c_2 = 1 - \lambda,$$

$$\sigma = \frac{\lambda^2}{1 + \lambda} = \frac{1}{2\cos\frac{1}{2}a}\exp(\tfrac{3}{2}i\alpha).$$

Thus the nonlinear terms of (2.5) can be derived from

$$z_{n+1} = \sigma[1 + (1-\bar{\lambda})z_n + (1-\lambda)\bar{z}_n)][z_n + \bar{z}_n - B(z_n+\bar{z}_n)^2 + C(z_n+\bar{z}_n)^3 + \cdots] + \ell_n, \tag{2.6}$$

where ℓ_n denotes linear terms. Without difficulty we read off the following expressions:

$$a_{20} = \sigma(1-\bar{\lambda}-B), \qquad a_{11} = \sigma(2-\lambda-\bar{\lambda}-2B), \qquad a_{02} = \sigma(1-\lambda-B),$$

and also $a_{21} = \sigma(\lambda + 2\bar{\lambda} - 3)B + 3\sigma C$. From the theory of normal forms the following formula can be derived:

$$\frac{\mu}{R^2} = \tfrac{1}{2}|a_{11}|^2 + |a_{02}|^2 - \operatorname{Re}\frac{(2-\bar{\lambda})a_{11}a_{20}}{\lambda(1-\lambda)} - \operatorname{Re}\,\bar{\lambda}a_{21}.$$

Substitution of the expressions for the coefficients obtained above gives the surprisingly simple result

$$\frac{2\mu}{R^2} = A - (A+1)B + 4B^2 - 3C, \tag{2.7}$$

where R is the radius of the Hopf circle in the coordinates $(z, \bar{z})$ of (2.3) and (2.5). However, in the original (x, y) coordinates, the Hopf circle is transformed into an invariant curve of elliptical shape. From (2.1) and (2.3) we obtain the local linear transformation

$$c\,\mathrm{d}z = \sigma[a(\bar{\lambda}-1)\,\mathrm{d}x + \mathrm{d}y] \tag{2.8}$$

written in local infinitesimal coordinates. The Hopf circle, small by nature, is given by

$$\mathrm{d}z\,\mathrm{d}\bar{z} = R^2,$$

where R^2 is determined by (2.7). Substitution of (2.8) gives an ellipse described in local infinitesimal coordinates $(\mathrm{d}x, \mathrm{d}y)$ by

$$a(a-1)\,\mathrm{d}x^2 - (a-1)\,\mathrm{d}x\,\mathrm{d}y + \mathrm{d}y^2 = (3a+1)c^2R^2/a.$$

Its position, semi-axes, etc. can be derived from this equation by standard analysis. However, no simple expressions can be obtained for the general case. Its area is given by

$$\frac{2\pi c^2R^2}{a}\left(\frac{3a+1}{a-1}\right)^{\frac{1}{2}},$$

perhaps the simplest formula of this kind.

It should be noted that a Hopf circle—or better—a Hopf ellipse, is merely an invariant curve in the (x, y) plane. For a starting point (x_0, y_0) on the Hopf curve, the two-dimensional dynamic behaviour of the model is reduced to one-dimensional dynamic behaviour. The motion can be aperiodic with a dense covering of the Hopf curve by successive points. However, if $\lambda = (1+\mu)\exp \mathrm{i}\alpha$ is close to a point of the unit circle with a low-order rational rotation number, i.e. if

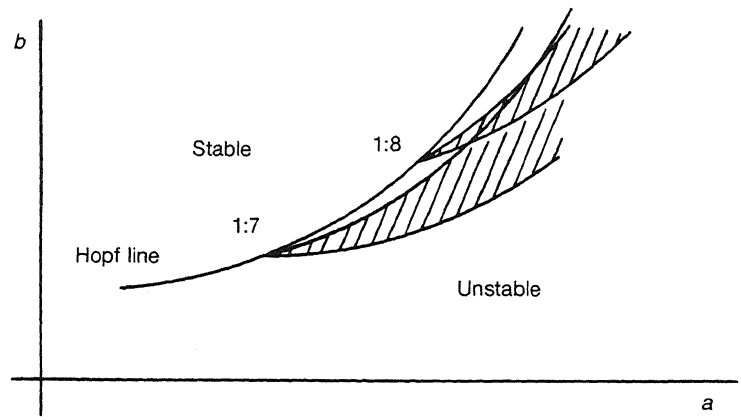

FIG. 1

$\alpha \approx m/n$, we may have periodic orbits. This is a case of weak resonance. The simplest cases are here 1 : 7, 1 : 8, 2 : 15, etc. According to Arnold, the regions in the parameter plane, for which a case of weak resonance occurs, have the shape of thin tongues or horns, with their pointed end at the Hopf line, and fanning well out in the unstable region. Tongues with a different rotation may even intersect each other. The general situation is sketched in Fig. 1.

We conclude this section by giving an alternative expression for the Hopf radius when the given model is of the form

$$x_{n+1} = x_n \exp[-f(y_n)], \qquad y_{n+1} = ax_n - x_{n+1}, \tag{2.9}$$

where

$$f(c(1+t)) = At + AB_1t^2 + AC_1t^3 + \ldots. \tag{2.10}$$

Then we have $B = \frac{1}{2}A - B_1$, $C = \frac{1}{6}A^2 - AB_1 + C_1$, and (2.7) passes into

$$\frac{2\mu}{R^2} = \tfrac{1}{2}A + B_1 + 4B_1^2 - 3C_1. \tag{2.11}$$

3. A simple model

In this section we consider the model

$$x_{n+1} = \frac{ax_n}{1+y_n^b}, \qquad y_{n+1} = \frac{ax_ny_n^b}{1+y_n^b}, \quad b > 0.$$

This is perhaps the simplest possible model, as we soon shall see. So we call it the S model (S = simple). The non-trivial equilibrium is given by

$$(a-1)^{1/b-1}, \qquad c = (a-1)^{1/b}. \tag{3.1}$$

The eigenvalue equation is $\lambda^2 - (1 + b/a)\lambda + b = 0$. Thus, in the (a, b) parameter plane, the regions of stability and instability are separated by the Hopf line $b = 1$.

The expansion

$$\phi(c(1+t)) = \frac{a}{a+ct} = 1 - \frac{ct}{a} + \frac{c^2t^2}{a^2} - \frac{c^3t^3}{a^3} + \dots,$$

with $c = a - 1$ on the Hopf line, gives $A = c/a$, $B = c/a$, $C = c^2/a$.
Substitution of these values in (1.5) gives $2\mu/R^2 = 0$, for all values of a. Thus we have no Hopf bifurcation in this case. Computer experiments suggest that, for $b < 1$, all orbits converge to the equilibrium (3.1) and that, for $b > 1$, all orbits disappear into infinity. For $b = 1$, we have the very simple model:

$$x_{n+1} = \frac{ax_n}{1+y_n}, \qquad y_{n+1} = \frac{ax_ny_n}{1+y_n}. \tag{3.2}$$

Its inverse is even simpler:

$$x_n = (x_{n+1} + y_{n+1})/a, \qquad y_n = y_{n+1}/x_{n+1}. \tag{3.3}$$

Computer experiments show that, for $a > 1$, the map (3.2) is very much like a Hamiltonian map. A few typical orbits are shown in Fig. 2. There are periodic cycles of any order from 9 upwards. In particular, the point $(x_0, y_0) = (0{\cdot}713, 2{\cdot}090)$ is an element of a 9-cycle, and $(0{\cdot}469, 3{\cdot}796)$ is an element of a 10-cycle. It is perhaps a surprise that on a logarithmic scale the map (3.3) is indeed Hamiltonian, i.e. area-preserving. With the variables u and v defined by

$$u = \log x, \qquad v = \log[y/(a-1)],$$

the map (3.3) takes the form

$$u \mapsto \log \frac{e^u + (a-1)e^v}{a}, \qquad v \mapsto v - u.$$

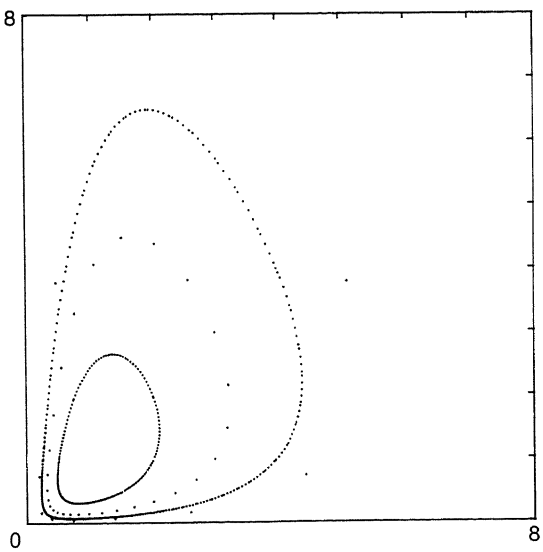

FIG. 2

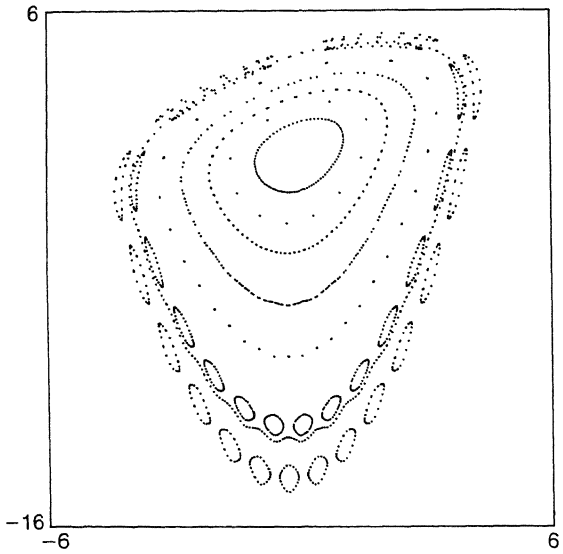

FIG. 3

In Fig. 3 an illustration is given, again for $a = 2$. An orbit consisting of an island chain is clearly visible. The parameter a is a sort of degree of stochasticity. As a increases, more and more orbits disintegrate into stochastic rings. An extreme case is shown in Fig. 4 for $a = 8$, where a single orbit is shown, starting from $(x_0, y_0) = (0, -20)$. Of course, such extreme situations have hardly any biological meaning.

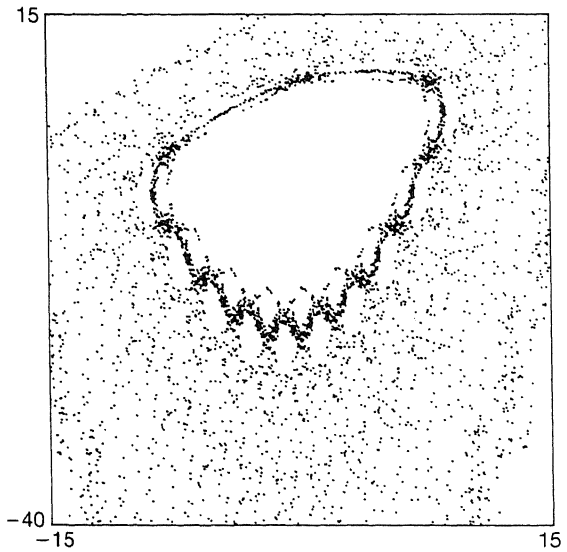

FIG. 4

4. The Hassel–Varley model

The HV model

$$x_{n+1} = ax_n \exp(-y_n^b), \qquad y_{n+1} = ax_n - x_{n+1}, \quad 0 < b \leqslant 1,$$

proposed by Hassell & Varley (1969), is a generalization of the Nicholson–Bailey model, to which it reduces for $b = 1$. The non-trivial equilibrium is here

$$(\log a)^{1/b}/(a-1), \qquad c = (\log a)^{1/b}.$$

The eigenvalue equation $(a-1)\lambda^2 - (a - 1 + b \log a)\lambda + ab \log a = 0$ shows stability for $ab \log a < a - 1$. The corresponding regions of stability and instability are sketched in Fig. 5. On the Hopf line the Taylor expansion of

$$f(c(1+t)) = [(1+t)^b - 1] \log a$$

gives, in the notation of (2.9, 2.10), the coefficients

$$A = b \log a, \qquad B_1 = \tfrac{1}{2}(b-1), \qquad C_1 = \tfrac{1}{6}(b-1)(b-2).$$

Then from (2.11) we obtain at once the simple result

$$\frac{4\mu}{R^2} = b^2 + b \log a - 1,$$

that is, expressed in terms of a alone,

$$\frac{\mu}{R^2} = \frac{(a-1)^2 - a \log^2 a}{4a^2 \log^2 a}.$$

Elementary calculus shows that, for $a > 1$, this expression is always positive. In Table 1 we have collected a few values of α, a, and b on the Hopf line, together with the equilibrium (x_0, y_0) and the quantity μ/R^2 determining the size of the Hopf curve. A typical orbit is given in Fig. 6.

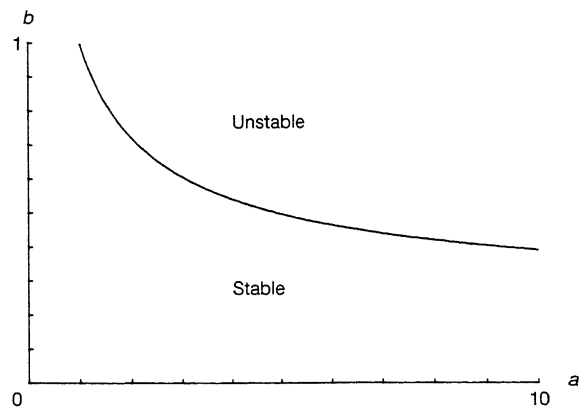

FIG. 5

TABLE 1

α	a	b	x_{eq}	y_{eq}	μ/R^2
30°	1·366	0·859	0·704	0·258	0·0015
40°	1·879	0·742	0·611	0·537	0·0045
45°	2·414	0·664	0·585	0·827	0·0069
50°	3·502	0·570	0·594	1·486	0·0098
53°	4·911	0·500	0·647	2·531	0·0117
56°	8·447	0·413	0·841	6·261	0·0131
59°	33·25	0·277	2·876	92·76	0·0117

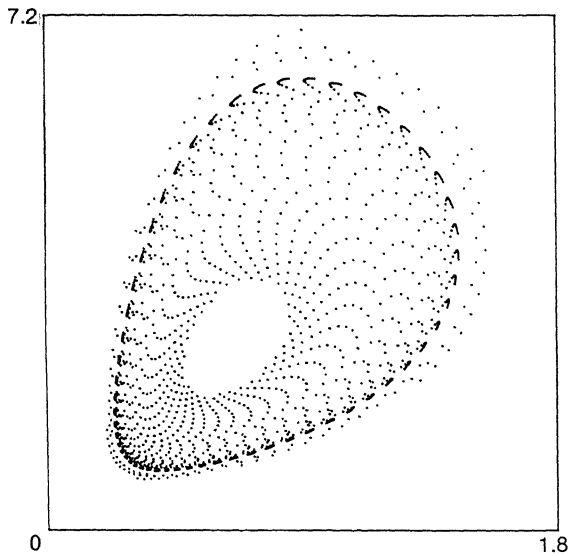

FIG. 6

5. The parasitoid–parasitoid interaction model

The PP model was specifically constructed to correct the unbiological property of the HV model, that at low parasitoid densities the pro capita search rate grows beyond bounds. We do not claim any realism in detail. The search rate of the PP model is finite at low parasitoid densities while at high parasitoid densities it behaves as the HV search rate with exponent $\frac{1}{2}$. The interesting point is that this added realism in the search-rate function leads to a behaviour which is, in certain respects, qualitatively different.

The PP model assumes that the parasitoids can be divided into two groups. The first group consists of single individuals looking for a host. The second group consists of pairs of parasitoids more interested in fighting each other. It is like a chemical reaction of the kind

$$P + P \rightleftharpoons P_2.$$

If u is the number of single parasitoids, v the number of competing pairs, so that $P = u + 2v$, then reaction kinetics requires an equation of the form

$$\dot{u} = -\alpha_1 u^2 + 2\alpha_2 v.$$

Equilibrium, on a small time scale, requires that $\alpha_1 u^2 - 2\alpha_2 v = 0$, i.e.

$$\alpha_1 u^2 + \alpha_2 u - \alpha_2 P = 0.$$

Solving this for u we have

$$2\alpha_1 u = -\alpha_2 + (\alpha_2^2 + 4\alpha_1\alpha_2 P)^{\frac{1}{2}}.$$

If this expression is used in combination with the Nicholson–Bailey model

$$x' = ax \exp(-u), \qquad y' = ax - x',$$

we obtain, after some scaling, the following so-called parasitoid–parasitoid interaction (PP) model

$$x' = ax \exp\left(-\frac{(1+y)^{\frac{1}{2}} - 1}{b}\right), \qquad y' = ax - x', \qquad b > 0.$$

For a small value of b, also x and y are small and then $(1+y)^{\frac{1}{2}} - 1 \approx \frac{1}{2}y$. This shows that, in that case, the model is very close to the Nicholson–Bailey model. If b is large, then also y is large, and then $(1+y)^{\frac{1}{2}} \approx y^{\frac{1}{2}}$. In that case the model is an approximation of the Hassell–Varley model with exponent $\frac{1}{2}$.

The non-trivial equilibrium is $(c/(a-1), c)$ with

$$c = (1 + b \log a)^2 - 1. \tag{5.1}$$

The eigenvalues follow from

$$\lambda_1\lambda_2 = \frac{a \log a(2 + b \log a)}{2(a-1)(1 + b \log a)}, \qquad \lambda_1 + \lambda_2 = 1 + \frac{\lambda_1\lambda_2}{a}.$$

The stability condition $\lambda_1\lambda_2 < 1$ can be written as

$$b > \frac{a}{2(a-1) - a \log a} - \frac{1}{\log a},$$

with $a < 4{\cdot}92155$, the value for which $2(a-1) = a \log a$. The corresponding regions of stability and instability are illustrated in Fig. 7. The vertical asymptote of the stability boundary corresponds to the stability switch of the HV model with exponent $\frac{1}{2}$. On the Hopf line, the Taylor expansion of

$$f(c(1+t)) = [(1 + c + ct)^{\frac{1}{2}} - (1+c)^{\frac{1}{2}}]/b$$

leads to the following expansion for the Hopf radius:

$$\frac{\mu}{R^2} = \frac{c}{8b(1+c)^{\frac{1}{2}}} - \frac{3c^2 + 2c}{16(1+c)^2}. \tag{5.2}$$

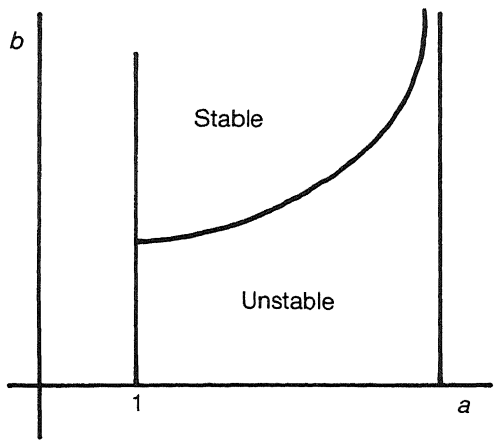

FIG. 7

On the Hopf line, the relations (5.1) and the relation

$$b = \frac{a}{2(a-1) - a \log a} - \frac{1}{\log a}$$

enable us to express μ/R^2 as a function of a only. Table 2 lists the results for some selected numerical values of α.

TABLE 2

α	a	b	x_{eq}	y_{eq}	μ/R^2
24°	1·209	1·144	2·302	0·481	−0·00399
30°	1·366	1·258	2·565	0·939	−0·00820
40°	1·879	1·695	3·733	3·283	−0·01556
45°	2·414	2·311	5·815	8·224	−0·01469
50°	3·502	4·897	19·96	49·94	−0·00401
51°	3·866	6·929	37·17	106·5	0·00016
52°	4·323	12·938	119·4	396·6	0·00530
53°	4·911	774·88	3·895E5	1·523E6	0·01159

It appears that here (5.2) changes sign at the critical value $\alpha = \alpha_0 = 50{\cdot}96°$. This means that, for $\alpha > \alpha_0$, we have supercritical Hopf bifurcation and, for $\alpha < \alpha_0$, subcritical Hopf bifurcation. According to the theory, for $\alpha > \alpha_0$ and α close to α_0, we may expect two invariant Hopf curves. The inner Hopf curve is attracting, and it is either densely filled by successive iteration points, or it contains a periodic cycle with a rotation number close to 1 : 7. The outer Hopf curve is repelling and separates the bounded orbits from the unbounded ones. A typical case is illustrated in Fig. 8 for $a = 4{\cdot}2$ and $b = 10$ corresponding to $\alpha = 51{\cdot}8°$ and $\mu = 0{\cdot}00156$. The equilibrium is at $(x, y) = (73{\cdot}3,\ 234{\cdot}6)$. The start (125, 929) gives the stable Hopf curve. The start (125, 1284) gives the separatrix, the unstable Hopf curve.

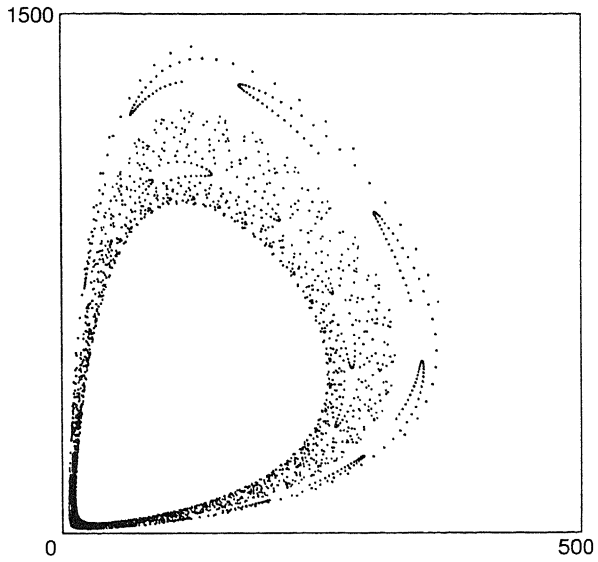

FIG. 8

6. Hassell's model

In his paper on parasitism in patchy environments Hassell considers the model

$$N_{n+1} = FN_n f(P_n), \qquad P_{n+1} = cN_n[1 - f(P_n)],$$

where $f(P) = \alpha e^{-\alpha\beta P} + (1-\alpha)e^{-g\alpha\beta P}$, with $g = \left(\frac{1-\alpha}{(n_0-1)\alpha}\right)^{\mu}$. Realistic values are

$$0{\cdot}3 \leqslant \alpha \leqslant 0{\cdot}6, \qquad n_0 \approx 10, \qquad F \approx 2, \qquad -3 \leqslant \mu \leqslant 3.$$

With the following scaling and change of notation,

$$N = Fx/\alpha\beta c, \qquad P = y/\alpha\beta, \qquad F = a, \qquad g = b, \qquad \alpha = \theta,$$

we obtain in our notation the model (1.1) with

$$\phi(y) = a[\theta e^{-y} + (1-\theta)e^{-by}], \qquad b > 0, \quad 0 < \theta < 1.$$

In view of the symmetry relations

$$x \to x/b, \qquad y \to y/b, \qquad \theta \to 1-\theta, \qquad b \to 1/b,$$

it is sufficient to consider only the case $b > 1$. The equilibrium of the model is determined by

$$a\theta e^{-c} + a(1-\theta)e^{-bc} = 1. \tag{6.1}$$

The product L of its eigenvalues is given by

$$L = \frac{a^2 c}{a-1}[\theta e^{-c} + (1-\theta)be^{-bc}]. \tag{6.2}$$

For given values of θ, α, and μ the corresponding values of a, b, and c can be determined by solving (6.1, 6.2), where

$$a = L/[2(1+\mu)\cos\alpha - 1], \qquad L = (1+\mu)^2.$$

Perhaps the simplest way of solving (6.1, 6.2) is as follows. We write

$$u = a\theta e^{-c}, \qquad v = a(1-\theta)e^{-bc},$$

and replace (6.1, 6.2) by

$$u + v = 1, \qquad u\log\frac{u}{\theta} + v\log\frac{v}{1-\theta} = \log a - \frac{a-1}{a}L,$$

with $u,v \in (0,1)$. Then we have to solve

$$f(u) \equiv u\log\frac{u}{\theta} + (1-u)\log\frac{1-u}{1-\theta} - \log a + L\frac{a-1}{a} = 0. \tag{6.3}$$

A possible root of $f(u)=0$ should result in a positive value of c and in $b>1$. This imposes the conditions $\theta < u < \theta a$. Since $df/du > 0$ for $\theta < u \leqslant 1$, the equation (6.3) yields a single root, provided

$$f(\theta) < 0, \qquad f(1) > 0 \quad \text{if } \theta a > 1, \qquad f(\theta a) > 0 \quad \text{if } \theta a < 1.$$

By these conditions in the (a, θ) plane a region of admissible values is determined. For $\mu = 0$ this region is sketched in Fig. 9. Its boundaries are determined by

$$\theta a = \exp\left(1 - \frac{1}{a}\right), \qquad a\log\left(1 + \frac{a-1}{1-\theta a}\right) = \frac{a-1}{1-\theta a}.$$

In particular, for $\theta = \frac{1}{2}$ we have $1 < a < 4{\cdot}3111$. The Hopf line in the (a,b)-

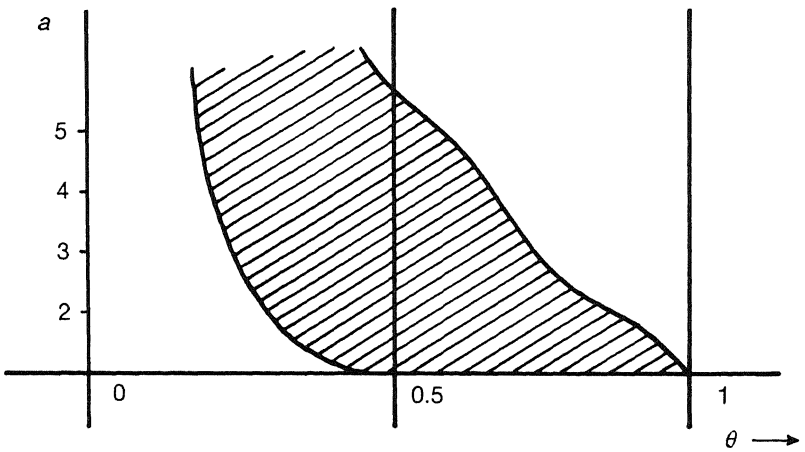

FIG. 9

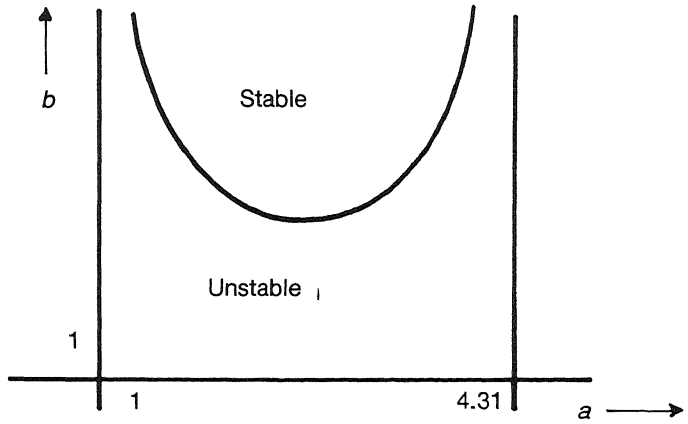

FIG. 10

parameter plane is determined by (6.3) with $L = 1$, i.e. by

$$u \log \frac{u}{\theta} + (1-u) \log \frac{1-u}{1-\theta} = \log a - \frac{a-1}{a}.$$

The corresponding illustration for the special case $\theta = \frac{1}{2}$ is given in Fig. 10. The expansion of the Hopf radius is determined by the Taylor expansion of

$$\phi(c(1+t)) = ue^{-ct} + ve^{-bct},$$

from which

$$A = c(u+bv) = 1 - 1/a, \qquad AB = \tfrac{1}{2}c^2(u+b^2v), \qquad AC = \tfrac{1}{6}c^3(u+b^3v).$$

Thus the same numerical procedure enables us to calculate (1.5). A few results are collected in Table 3 for this case $\theta = \frac{1}{2}$.

The expression of the Hopf radius changes sign at $\alpha = 44{\cdot}05°$ ($a = 2{\cdot}286$) and at $\alpha = 51{\cdot}79°$ ($a = 4{\cdot}220$) close to the boundary $\alpha = 51{\cdot}977°$ ($a = 4{\cdot}311$). This means that close to the Hopf line we have two regions of supercritical Hopf bifurcation and subcritical Hopf bifurcation for $44{\cdot}05° < \alpha < 51{\cdot}79°$. Close to the boundaries $\alpha \approx 2{\cdot}29$ and $a \approx 4{\cdot}22$ we have anomalous Hopf bifurcation with two

TABLE 3

α	a	b	x_{eq}	y_{eq}	μ/R^2
24°	1·209	18·373	0·102	0·021	0·01035
30°	1·366	12·247	0·147	0·054	0·02376
40°	1·879	7·600	0·216	0·190	0·03931
45°	2·414	6·531	0·236	0·334	−0·02068
48°	2·956	6·282	0·241	0·471	−0·12926
50°	3·502	6·521	0·238	0·597	−0·21569
51°	3·866	7·096	0·236	0·675	−0·19912
51.9°	4·272	10·285	0·232	0·760	0·08046

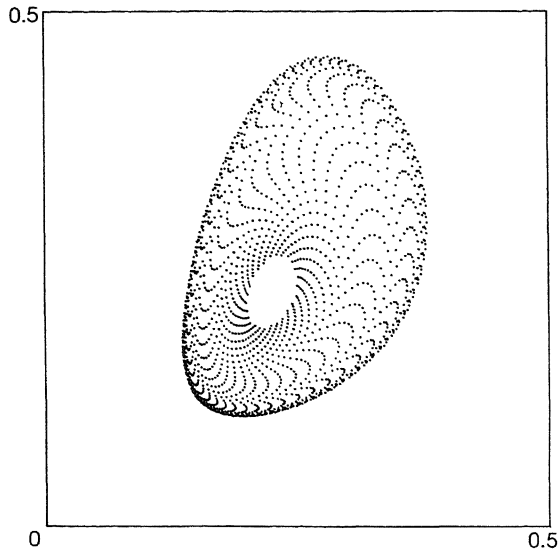

FIG. 11

Hopf curves. A typical case is given in Fig. 11 for $\theta = 0{\cdot}5$, $a = 2$, $b = 7{\cdot}1$. In this case there is an attracting Hopf curve and a second unstable Hopf curve separating the bounded and the unbounded orbits. The corresponding position on the Hopf line is $a = 2$ with $b = 7{\cdot}231$. For $a = 2$ and $b = 7{\cdot}06$, the two Hopf curves coalesce, annihilating each other. Thus, for $a = 2$ and $b < 7{\cdot}06$, all orbits are unbounded.

7. Discussion

Mathematically, it is surprising that a seemingly rather complicated class of iterative processes yields such pleasingly simple formulae for its Hopf bifurcations. So-called transcritical Hopf bifurcations, i.e. Hopf bifurcations which switch from being supercritical to being subcritical, or vice versa, have recently attracted a great deal of attention (e.g. Chenciner, 1983). The main interest is the complicated interactions of the Arnold tongues with the 'crater rim'. We hope soon to present a more detailed account of our numerical explorations of these phenomena for the PP model.

Biologically, the two most interesting results are the period-larger-than-six theorem from the introduction, and the gross phenomena accompanying the transcritical Hopf bifurcation.

Some care is needed in interpreting the period-larger-than-six result. 'Period'—in the strict mathematical sense—entails returning to exactly the same point after so many iterations. In the 2 : 15 Arnold tongue we may encounter period-fifteen oscillations, but these go round the Hopf circle twice. Biologically we are seeing 'period $7\frac{1}{2}$'. Moreover, it is only this biological period which remains visible when

slightly more than the tiniest amount of noise is added. We specifically formulated the theorem such that it applies to both concepts of period.

The presence of transcritical Hopf bifurcation has consequences for the domains of attraction of either the equilibrium or the stable Hopf circle. For example, in the PP model both the stable equilibrium and the stable Hopf circle are always surrounded by an unstable Hopf circle bounding their domains of attraction. If we start too far away from the equilibrium we see ever increasing oscillations just as in the Nicholson–Baily model. When we let b go to infinity so that the PP model goes to the HV model, the area inside the unstable circle grows larger and larger and it appears as if, in the limit, the circle disappears by moving off towards infinity or merging with the axes. However, the fact that the circle is clearly there for smaller values of b should instill a little caution in dealing with the HV model: it is apparently only the unrealistic behaviour, of the search-rate function near zero parasitoid density, assumed in the HV model, which makes for the simple character of its Hopf bifurcation.

Acknowledgements

The occurrence of the transcritical Hopf bifurcation in the PP model was first discovered numerically by Marlies Vaz Nunez. Jan Willem Lubberhuizen did many numerical calculations on Arnold tongues for both the HV and PP model, leading to the extended version of the period-larger-than-six theorem mentioned in the text.

REFERENCES

CHENCINER, A. 1983 Bifurcations de difféomorphisms de $\mathbb{R}^2$ au voisinage d'un point fixe ellyptique. In: G. Iooss & H. G. Helleman (Eds), *Les Houches Ecole d'Eté de Physique Théorique.* North Holland, Amsterdam.

HASSELL, M. P. 1978 The Dynamics of Arthropod Predator–Prey Systems. Princeton.

HASSELL, M. P. 1984 Parasitism in patchy environments. *IMA J. Math. appl. in Med. & Biol.* **1,** 123–133.

HASSELL, M. P., & VARLEY, G. C. 1969 New inductive population model for insect parasites and its bearing on biological control. *Nature* **223,** 1133–1137.

LUBBERHUIZEN, J. W. P. 1983 De misdragingen van een model. Internal report, Institute of Theoretical Biology, Leiden.

VAZ NUNEZ, M. 1977 Limietcycli in het parasitoid-gastheer model van Hassell–Varley en een modificatie daarvan. Internal report, Institute of Theoretical Biology, Leiden.

Appendix

In this appendix, a theory is given of normal and anomalous Hopf bifurcation. Our starting-point is the following normal form in complex coordinates $(z, \bar{z})$ where $z = x + \mathrm{i}y$ or $z = r \exp \mathrm{i}\theta$ in polar coordinates

$$z' = \lambda z - Qz^2\bar{z} + \hbar, \tag{A.1}$$

with $\lambda = (1 + \mu)\mathrm{e}^{\mathrm{i}\alpha}$ and $\hbar$ generically denoting higher-order terms. By suitable scaling it can be arranged that $|Q| = 1$. Accordingly, we write

$$Q = \exp \mathrm{i}\gamma.$$

From (A.1) we obtain, for the square modulus $s = r^2 = z\bar{z}$, the transformation

$$s' = (1 + 2\mu)s - 2\cos(\alpha - \gamma)s^2 + \hbar,$$

where $\hbar$ contains all terms of order μ^3 and higher, assuming that $s = O(\mu)$. For $s' = s$, we obtain the well-known relation for the radius of the Hopf circle:

$$s = \mu/\cos(\alpha - \gamma),$$

i.e.

$$\mu/R^2 = \cos(\alpha - \gamma).$$

If $\cos(\alpha - \gamma)$ is not small, we obtain either supercritical or subcritical Hopf bifurcation depending on the sign of $\cos(\alpha - \gamma)$. However, if $\cos(\alpha - \gamma)$ is small, the analysis breaks down. It becomes necessary to extend the normal form (A.1) by taking

$$z' = \lambda z - Qz^2\bar{z} + Q_1 z^3\bar{z}^2 + O(z^6).$$

This normal form holds when lower resonances up to the order 6 are excluded. Fortunately, this is no restriction in the host–parasitoid models. Proceeding as before, we have for $s = r^2$ the transformation

$$s' = (1 + 2\mu)s - 2\cos(\alpha - \gamma)s^2 + Cs^3 + \hbar,$$

where $C = 1 + e^{i\alpha}\bar{Q}_1 + e^{-i\alpha}Q_1$. For an invariant circle we should have $s' = s$. This gives, at the lowest order of approximation, the quadratic equation

$$Cs^2 - 2s\cos(\alpha - \gamma) + 2\mu = 0, \tag{A.2}$$

giving $Cs = \cos(\alpha - \gamma) \pm [\cos^2(\alpha - \gamma) - 2\mu C]^{\frac{1}{2}}$. Depending on the signs of μ, C,

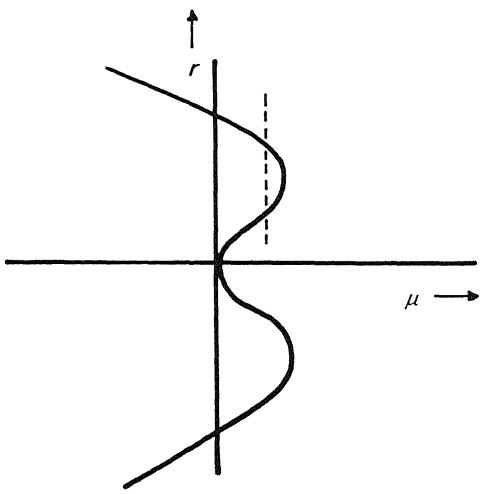

FIG. 12

and $\cos(\alpha - \gamma)$, there may be two roots, giving two Hopf circles. One of the possibilities is sketched in the bifurcation diagram of Fig. 12. The bifurcation line is determined by (A.2) with $s = r^2$. If $\mu > 0$ and sufficiently small, we have two Hopf circles. It can be shown that the inner circle is stable and that the outer one is unstable. If μ increases gradually, the two circles approach each other, coalesce, and disappear.